Ab initio study on structural and electronic properties of Ba_nO_m clusters

G. Chen
Institute of Solid State Physics, Chinese Academy of Sciences, 230031-Hefei, P. R. China and Interdisciplinary Center of Theoretical Studies, Chinese Academy of Sciences, 100080-Beijing, People's Republic of China

Z. F. Liu
Department of Chemistry, Chinese University of Hong Kong, Shatin, Hong Kong, People's Republic of China

X. G. Gong[a)]
Surface Physics Laboratory and Department of Physics, Fudan University, Shanghai 200433, China and Institute of Solid State Physics, Chinese Academy of Sciences, 230031-Hefei, People's Republic of China

(Received 2 December 2003; accepted 11 February 2004)

Density-functional calculation within local density approximation, shows that the electronic property of a barium oxide cluster is strongly correlated with its equilibrium structure. The ground-state structures of Ba_nO_m $(4 \leqslant n \leqslant 9, m \leqslant n)$ clusters can be classified into four categories: (a) compact, (b) dangling state, (c) *F—center*, and (d) stoichiometric. The compact cluster is metallic, almost no energy gap exists between the highest occupied and the lowest unoccupied molecular orbitals. The energy gap for the dangling state cluster is larger than that for the *F—center* cluster, while the stoichiometric cluster has the largest energy gap. © *2004 American Institute of Physics.* [DOI: 10.1063/1.1691785]

I. INTRODUCTION

The study on oxidation phenomenon is important to the application of metal material. Either for bulk or for surface, there remains much to be understood about the mechanism of metal oxidation. Clusters bridge the gap between individual atoms or molecules and the bulk condensed state. Studies on the oxidation of metal clusters, especially on the evolution of structural and electronic property with increasing oxygen content can provide us with valuable insights into the oxidation processes. In the past few years, a number of studies on alkali oxide clusters have been reported,[1–4] in which segregation and shell closing effect were observed. The atomic structure could be viewed as $M_n(M_2O)_m$, where M stands for alkali atom. In other words, the excess alkali atoms aggregate among themselves to form a cluster M_n, which is capped by a stoichiometric $(M_2O)_m$ cluster. In the stoichiometric part, the alkali valence electrons are localized in the bonds interacting with oxygen atoms. In the metal cluster part, the alkali valence electrons are delocalized and responsible for a magic size when these electrons fill up the bonding shells.

An alkaline–earth metal atom differs from an alkali atom in that it has a closed shell of ns^2 and the electronic properties of alkaline–earth clusters are distinct from their alkali cousins. Dimers,[5–8] such as Mg_2 and Ba_2 are weakly bonded by the van der Waals interaction, even though the alkaline–earth elements in solid state are well-known metals. Theoretical calculations show that a transition from van der Waals to metallic interaction takes place soon after the cluster size increased above 2.[6–9] Alkaline–earth oxides are of particular interest since, by varying the content of metal atoms and oxygen atoms in clusters, one could observe the metallic to ionic transition. Studies on stoichiometric clusters, such as $(MgO)_n$,[10–12] $(CaO)_n$,[15] and $(BaO)_n$,[16] showed the ionic cubiclike structures to be ground states, as governed by ionic bonds between metal atoms and oxygen atoms, although other structures were also possible to be energy favorable in small clusters.[11–14] By contrast, less is known about metal-rich clusters. With mass spectra of alkaline–earth oxide clusters, Martin *et al.*[15] found that, the magic numbers for the icosahedral Ba_n clusters do not change upon the uptake of a small number of O atoms ($\leqslant 5$), which indicates that the structure of the icosahedral Ba_n could embed a few O atoms. Based on results obtained by one-photon ionization technique along with mass spectrometry, Boutou *et al.* predicted a structural transition upon further uptake of oxygen atoms.[17,18]

In order to understand in details the effect of oxygen on the barium clusters and to explain the experimental observations, we have performed first-principles studies on barium oxide clusters. For stoichiometric barium oxide clusters, the electronic effect is important, with three modes of growth: cubiclike, ringlike, and anti-tetragonal prism based. Although the cubiclike structure is the most stable, the total energy difference between the cubiclike structure and other isomeric structures is small.[16] Starting from bare Ba_n clusters, the structural evolution of Ba_nO_m with increasing oxygen content was also studied.[19] A transition from compact to cubiclike structure was observed, which disrupted the frame of bare Ba_n cluster, in agreement with experimental results. Such structural changes of the clusters will undoubtedly lead to a corresponding change in electronic properties, which is important however has not been fully understood yet. As a further efforts to understand such transition, we have calculated the evolution of electronic property of cluster Ba_nO_m and its relationship with geometrical structure, during the

a)Electronic mail: xggong@fudan.edu.cn

uptake of oxygen atoms by barium clusters, based on an extensive study of Ba_nO_m, using the plane-wave/pseupotential based density-functional theory (DFT) method. The optimized structures fall into four categories, with distinct electronic properties, underlying the gradual transition from metallic to ionic bonding during the oxidation process.

II. DETAILS OF CALCULATIONS

The density functional theory with local density approximation is a well established tool to study the structural and electronic properties of materials.[20,21] In the present studies, we adopt a powerful *ab initio* molecular-dynamics method with plane-wave basis.[22] The total free energy is variational quantity. The fully nonlocal optimized ultrasoft pseudopotential established by Vanderbilt[23] is used to describe the interaction between the core and valence electrons. The exchange-correlation energy of valence electrons is described by the local density functional approximation developed by Mermin.[24] The clusters with size $n \leqslant 5$ are placed in a simple cubic cell with edge length 16 Å, while a bigger cell with edge length 18 Å is used in calculations of clusters with size $6 \leqslant n \leqslant 9$. The size of the cell is large enough that the interaction between a cluster and its periodic images is negligible. Only the Γ point is considered for *k—point* sampling to represent the Brillouin zone in such large cell. The cut-off energy is set at 270.0 eV in the plane-wave expansion of the wave functions, which is large enough to obtain a good convergence.

For lack of *a priori* information about its shapes of the clusters, we performed an extensive sampling of the potential energy surface by generating a large set of random configurations for each Ba_nO_m cluster $(m \leqslant n \leqslant 9)$. From each initial configuration, the structures is optimized by the conjugated gradient iterative minimization method,[21] with a force convergence up to 0.02 eV/Å. Then the lowest total energy is adopted as the ground state. Based on these obtained structures, we have studied their electronic properties in details.

III. RESULTS AND DISCUSSIONS

In order to test the accuracy of our methods, we have optimized interatomic distances of the Ba_2, BaO, O_2, respectively. The obtained interatomic distances are 4.96, 2.22, and 1.30 Å, respectively, which are in agreement with other theoretical results.[5,17,25,26] We have also calculated the lattice constants of *bcc* Ba crystal and NaCl-like BaO crystal. The calculated lattice constants are 4.88 and 5.54 Å, respectively, which are in good agreement with the experimental results, 5.02 Å for Ba crystal and 5.54 Å for BaO crystal.[27,28]

Figure 1 shows the optimized equilibrium structures of Ba_nO_m clusters with size $n \leqslant 3$. Since there are just a few Ba atoms and O atoms, the quantum effect plays an important role. Present theoretical study shows that plane structures of clusters Ba_2O, Ba_2O_2, and Ba_3O are energetically favorable. The optimized equilibrium interatomic distance and cohesive energy for BaO molecule are 2.22 and 7.41 eV, respectively. Using molecular dynamics, we found that the vibration frequency ω_e of BaO molecule is 709 cm^{-1}, which is 6% larger than the experimental result.[28] Meanwhile an isosceles triangle and a rhombus configuration are found to be ground states of Ba_2O and Ba_2O_2, respectively. As studied previously,[6] Ba_3 forms an equilateral triangle. The doped O atom of Ba_3O is found localized at the center of the equilateral triangle. The three-dimensional structure begins at Ba_3O_2 with C_{3v} symmetry. The stoichiometric cluster Ba_3O_3 has a low symmetry structure, as presented in Fig. 1.

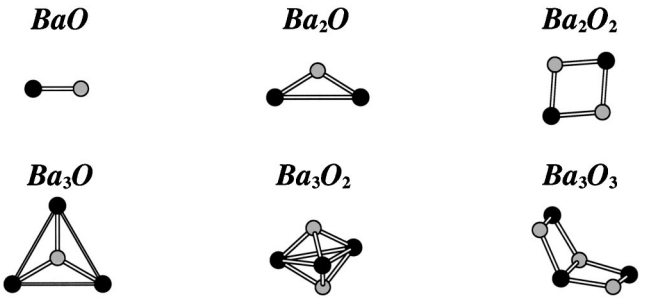

FIG. 1. Equilibrium structures of Ba_nO_m $(m \leqslant n \leqslant 3)$ clusters. Dark circle for Ba atom and gray circle for O atom.

The bare Ba_n cluster could accommodate a few O atoms while keep its compact structure unchanged, as discussed previously.[19] With the oxygen content increasing, a structural transition from compact structure to cubiclike structure occurs at $n-m=4$. According to the structural characters of the optimized clusters, we could generally classify the clusters into four categories: (a) Compact structure cluster (CSC), which reserves the bare Ba_n structure frame with oxygen atoms at the interstitial positions, as shown in Fig. 2(a); (b), dangling state cluster (DSC), which keeps a complete cuboid core fraction in its structure, with excess Ba atoms dangling upon it, as illustrated in Fig. 2(b); (c), *F—center* cluster (FC), with one oxygen atom missing from the corner of a cuboid core, as presented in Fig. 2(c), and (d), stoichiometric cluster (SC), which has a cubiclike structure without any excess Ba atoms while the stoichiometric condition is kept.

Among above four categories, the structures of CSC and SC clusters are very much different, CSC is for the barium-riched cluster, while SC is for the stoichiometric cluster. However, both DSC and FC clusters appear in the region $1 \leqslant n-m \leqslant 4$. Since the formation of the first cuboid needs four oxygen atoms, while the additional cuboid needs only two oxygen atoms, all the dangling state clusters have even number of oxygen atoms. For the cluster with an odd number of oxygen atoms, there is no way to form cuboid, there must be a oxygen atom missing at the corner, i.e., resulting in *F—center*. However, we find two FC clusters, Ba_8O_6 and Ba_9O_8, which have even number of oxygen atoms. For Ba_8O_6 cluster, we can see two missing oxygen atoms, i.e., two *F—centers* are included. In fact, the DSC structure of Ba_8O_6 has almost the same energy as the *F—center* structure. The Ba_9O_8 cluster should also be a DSC structure if the eighth oxygen atom takes the *F—center* position in Ba_9O_7 cluster, however, the cluster shape transition, from $4\times2\times2$ to $3\times3\times2$, takes place, as the eighth oxygen atom is attached to Ba_9O_7, thus one *F—center* is still left there.

All four kinds of structures have their own characteris-

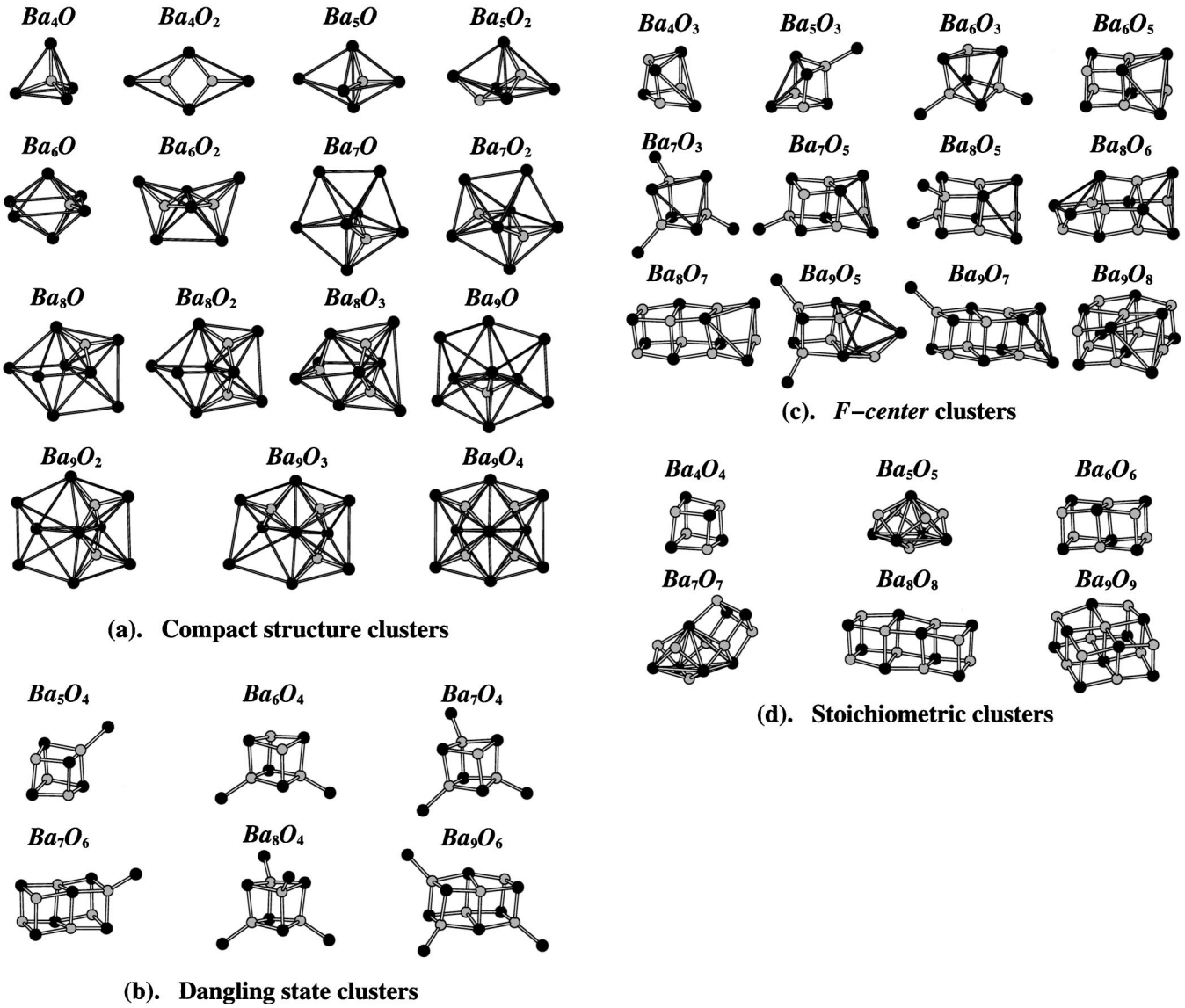

FIG. 2. Equilibrium structures of Ba_nO_m ($m \leqslant n, 4 \leqslant n \leqslant 9$) clusters. Dark circle for Ba atom and gray circle for O atom. (a) Compact structure clusters; (b) dangling state clusters; (c) *F—center* clusters; and (d) stoichiometric clusters.

tics of the electronic structures. Figure 3 shows the charge density of the highest occupied molecular orbital (HOMO) of CSC, DSC, FC, and SC. In CSC Ba_4O, the electrons in HOMO are mainly distributed on the surface of the tetrahedron frame, which shows that the metallic binding property of Ba_4 cluster is kept unchanged. We have also explored the localization of electrons of Ba_4O cluster, using the electron localization function (ELF) analysis,[29,30] which was introduced in quantum chemistry to measure the parallel spin correlation by defining conditional probability of finding an electron in the neighborhood of another electron with the same spin. ELF is defined as

$$\mathrm{ELF} = \frac{1}{1+[D/D_h]^2}, \tag{3.1}$$

$$D = \frac{1}{2}\sum_i |\nabla \phi_i|^2 - \frac{1}{8}\frac{|\nabla \rho|^2}{\rho}, \tag{3.2}$$

$$D_h = \frac{3}{10}(3\pi^2)^{2/3}\rho^{5/3}, \tag{3.3}$$

where ϕ_i is the Kohn–Sham orbital, and ρ is the local density. Most of ELF data surrounding Ba_4O are around 0.55, and no datum is larger than 0.80, which confirms the metallic bonding property. Therefore, the compact structure of bare Ba_4 cluster is preserved in low oxygen content CSC Ba_4O. Figure 3 also shows the HOMO charge distribution of DSC Ba_6O_4. The HOMO charge is mostly distributed around the dangling barium atoms. Ba_8O_5 cluster is a *F—center* cluster, the HOMO electrons are mainly localized at the vacancy where an oxygen atom missed, which is analogy to the *F—center* in bulk material. In the stoichiometric cluster of Ba_8O_8, the binding is completely ionic, the HOMO is essentially the $2p$ orbits of oxygen atoms, it is not surprising to find that all charge of HOMO is localized on O atoms, as shown in the figure.

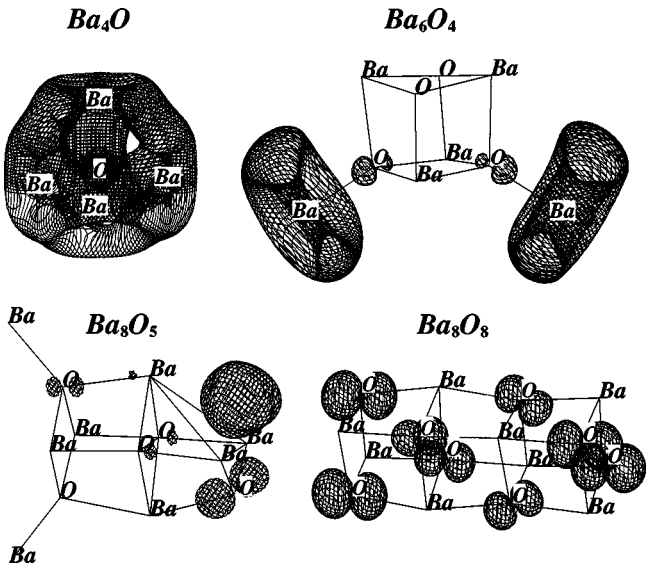

FIG. 3. Partial band decomposed charge density of HOMO, 0.000 02 $Å^{-3}$ spacing for Ba_4O and Ba_6O_4, 0.000 04 $Å^{-3}$ spacing for Ba_8O_5 and Ba_8O_8. The excess HOMO charge is distributed on the surface of compact structure cluster Ba_4O, mainly located in the vacancy of *F—center* cluster Ba_8O_5, and is distributed around the dangling barium cations of dangling state cluster Ba_6O_4. For stoichiometric cluster Ba_8O_8, the HOMO charge is bonded at O atoms.

The energy gap between HOMO and the lowest unoccupied molecular orbital (LUMO) is shown in Table I, it can be seen that the energy gap can be correlated with the structural characteristics. From the structures of Ba_n clusters reported previously,[6] we also calculated the energy gaps of Ba_n clusters, which are around 0.3 eV. In CSC, besides a small part of the valence electrons of the clusters are localized by the oxygen atoms, the number of the other valence electrons is big to keep the metallic binding property unchanged, thus the energy gap of CSC is very small. When uptaking more O atoms, the Ba_n structure frame will change and then the cubiclike structure growth mode begins. In DSC, FC, and SC, O atoms can attract enough valence electrons from Ba atoms, resulting in a significant energy gap. However, it is interesting to note that DSC has *s* electrons on dangling barium atoms, but no bonds exist between these well-separated barium atoms. In FC, some valence electrons are localized at *F—center*. Thus the DSC and FC show a significant energy gaps in the range of 0.7–1.2 eV. Finally, in SC cluster, the bonding is fully ionic, with the largest energy gap of ~2.3 eV. Although, generally the different structure category has its own typical value of energy gap, we can also find exceptions, for instance some *F—center* clusters have band gaps typical of compact clusters.

In order to give a more detailed description of the electronic properties, we have calculated the density of states (DOS) as shown in Fig. 4. It is obvious that almost no energy gap appears for the bare Ba_n cluster. When an O atom doped, some electronic bands could be observed with energies

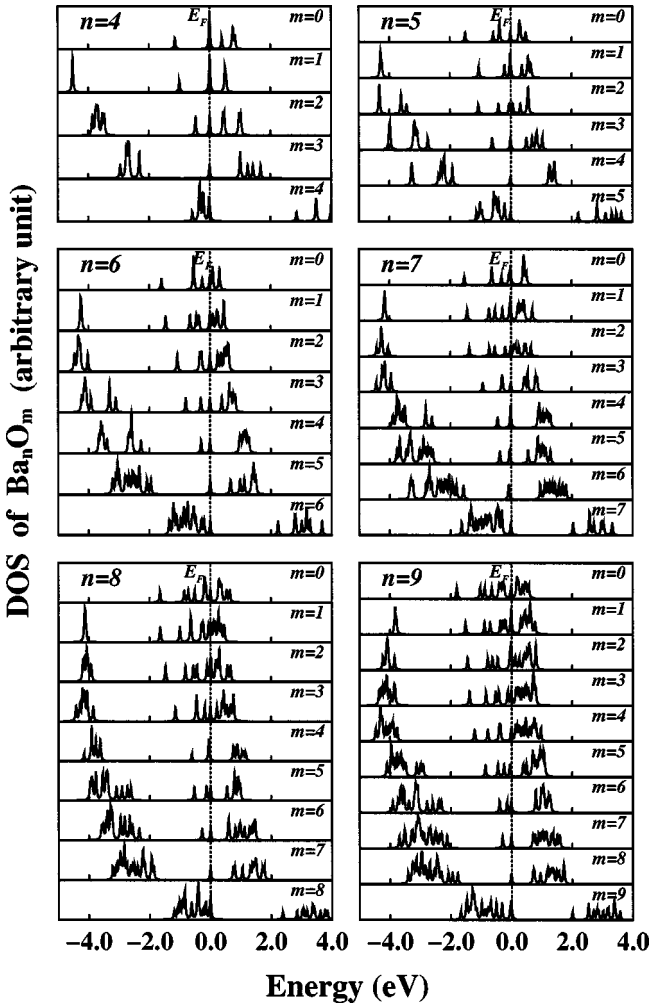

FIG. 4. Density of states of Ba_nO_m ($m \leqslant n, 4 \leqslant n \leqslant 9$) clusters. The *Fermi* energy is shifted to zero and marked by dotted line.

TABLE I. The calculated energy gap (eV) and the vertical ionization potential (IP_v) (eV). Only those structures plotted in Fig. 2 are presented.

Category	Cluster	Gap	IP_v	*Category*	Cluster	Gap	IP_v
Ba_n[a]	Ba_4	0.41	3.18	DSC	Ba_7O_4	0.90	2.82
	Ba_5	0.30	2.84		Ba_7O_6	1.05	2.99
	Ba_6	0.09	2.74		Ba_8O_4	0.80	2.83
	Ba_7	0.42	2.78		Ba_9O_6	0.80	2.60
	Ba_8	0.27	2.67	FC	Ba_4O_3	1.01	2.79
	Ba_7O_2	0.61	2.58		Ba_7O_5	0.61	2.58
CSC	Ba_4O	0.50	2.80		Ba_6O_3	0.39	2.66
	Ba_4O_2	0.44	2.68		Ba_6O_5	0.67	2.64
	Ba_5O	0.38	2.82		Ba_7O_3	0.43	2.73
	Ba_5O_2	0.12	2.48		Ba_7O_2	0.61	2.58
	Ba_6O	0.10	2.64		Ba_8O_5	0.54	2.59
	Ba_6O_2	0.25	2.75		Ba_8O_6	0.59	2.38
	Ba_7O	0.23	2.64		Ba_8O_7	0.75	2.52
	Ba_7O_2	0.10	2.48		Ba_9O_5	0.44	2.52
	Ba_8O	0.08	2.48		Ba_9O_7	0.71	2.46
	Ba_8O_2	0.03	2.41		Ba_9O_8	0.72	2.38
	Ba_8O_3	0.22	2.58	SC	Ba_4O_4	2.86	5.11
	Ba_9O	0.31	2.59		Ba_5O_5	2.22	4.63
	Ba_9O_2	0.14	2.54		Ba_6O_6	2.24	4.48
	Ba_9O_3	0.15	2.43		Ba_7O_7	2.05	4.31
	Ba_9O_4	0.14	2.39		Ba_8O_8	2.38	4.33
DSC	Ba_5O_4	1.27	3.04		Ba_9O_9	2.01	4.00
	Ba_6O_4	0.97	2.83				

[a]The energy gap and IP_v are calculated based on the structures presented in Ref. 6.

~4 eV below *Fermi* energy, which relates to the O $2p$ bands. At the first oxidation stage of Ba_n cluster, the uptaking of O atoms does not alter the energy gap significantly, this is strongly correlated with its metallic binding property. The energies of O $2p$ bands do not change much. Along with the uptaking of O atoms, the compact structure frame breaks, a large energy gap appears. When doped more O atoms, the energy difference between O $2p$ bands and the *Fermi* energy decreases. When the stoichiometric condition is reached, all the valence electrons of Ba atoms are transfered to the O atoms to form strong ionic bonds. Energy difference between the bands related to O $2p$ bands and the *Fermi* energy disappears. An energy gap of about 2.3 eV is opened, which indicates that the binding property has evolved to completely ionic.

The vertical ionization potential (IP_v) of Ba_nO_m and bare Ba_n clusters is shown in Table I. The vertical IP_v is defined as the energy difference between the charged and neutral cluster, while the structure of charged cluster is constrained to that of the ground state of the neutral cluster. In bare Ba_n clusters, *s* electrons form the metallic bonds, the IP_vs are 3.2–2.6 eV, depending on the size of the clusters. In the CSC cluster where a few oxygen atoms are doped in, two localized electrons on each oxygen atom increase the repulsive interaction among the valence electrons, the IP_vs slightly decrease as shown in Table I. It seems that Ba_9O and Ba_9O_2 are exceptional, this is because the structure of Ba_9 is very compact. The doping of oxygen expands the structure. When more and more oxygen atoms are added into the barium clusters, the structures become DSC. In such DSC cluster, HOMO electrons become more or less localized on the barium atoms which is dangling to the central cuboid (Fig. 3), the IP_vs increase a little from CSC structure. While in the *F—center* cluster, the HOMO electrons are weakly bonded near the site of the *F—center*, so we get a slight decrease of IP_v from DSC clusters. It is not surprising to find that SC clusters have a very large IP_v, due to the fully ionic bonds in the whole cluster. Our results are qualitatively in agreement with experimental data,[16] however, there is a systematic error of ~0.5 eV, which might be due to image interaction in the charged clusters.

IV. CONCLUSIONS

In summary, we have performed an extensive theoretical study on the electronic property and the atomic structure of Ba_nO_m cluster. According to the geometry of the clusters, we have divided equilibrium structures into four categories, CSC, DSC, FC, and SC. The results show that, the electronic property of cluster is strongly correlated with the ground-state structure. The metallic binding property of CSC is kept unchanged when doped O atoms. In DSC, the HOMO electrons are distributed around the dangling barium atoms. The energy gap is found to be 0.8–1.2 eV. FC has a missing atom in their structure, in which HOMO electrons mainly play the role of the missing O^{2-} anion, and the energy gap is smaller than that of DSC. We also find that the calculated IP_v of FC cluster is lowest and that of the SC cluster is largest among all the four kinds of clusters. The obtained relationship between the calculated IP_v and the structure is in very good agreement with the theoretical study on sodium fluoride clusters.[31,32]

ACKNOWLEDGMENTS

One of the authors (G. Chen) wishes to thank D. Y. Sun, X. M. Duan, and S. P. Chan for the stimulating discussions. This work is supported by the National Science Foundation of China, the special funds for major state basic research and CAS projects. Z. F. Liu also acknowledges financial supports from The Research Grant Council, Hong Kong SAR Government, through Project CUHK 4188/97P.

[1] P. Lievens, P. Thoen, S. Bouckaert, W. Bouwen, F. Vanhoutte, H. Weidele, and R. E. Silverans, J. Chem. Phys. **110**, 10316 (1999).
[2] N. Malinowski, H. Schabler, T. Bergmann, and T. P. Martin, Solid State Commun. **69**, 733 (1989).
[3] T. Bergmann, H. Limberger, and T. P. Martin, Phys. Rev. Lett. **60**, 1767 (1988).
[4] T. Bergmann and T. P. Martin, J. Chem. Phys. **90**, 2848 (1989).
[5] V. Boutou, A. R. Allouche, F. Spiegelmann, J. Chevaleyre, and M. A. Frécon, Eur. Phys. J. D **2**, 63 (1998).
[6] G. Chen, Z. F. Liu, and X. G. Gong, Eur. Phys. J. D **16**, 33 (2001).
[7] V. Kumar and R. Car, Phys. Rev. B **44**, 8243 (1991).
[8] R. Kawai and J. H. Weare, Phys. Rev. Lett. **65**, 80 (1990).
[9] X. G. Gong, Q. Q. Zheng, and Y. Z. He, Phys. Lett. A **181**, 459 (1993).
[10] P. J. Ziemann and A. W. Castleman, Jr., Phys. Rev. B **44**, 6488 (1991).
[11] W. A. Saunders, Phys. Rev. B **37**, 6583 (1988).
[12] P. J. Ziemann and A. W. Castleman, Jr., J. Chem. Phys. **94**, 718 (1991).
[13] A. Aguado and J. M. López, J. Phys. Chem. B **104**, 8398 (2000).
[14] C. Roberts and R. L. Johnston, Phys. Chem. Chem. Phys. **3**, 5024 (2001).
[15] T. P. Martin and T. Bergmann, J. Chem. Phys. **90**, 6664 (1989).
[16] G. Chen, Z. F. Liu, and X. G. Gong, J. Chem. Phys. **116**, 1339 (2002).
[17] V. Boutou, M. A. Lebeault, A. R. Allouche, C. Bordas, F. Paulig, J. Viallon, and J. Chevaleyre, Phys. Rev. Lett. **80**, 2817 (1998).
[18] V. Boutou, M. A. Lebeault, A. R. Allouche, F. Paulig, J. Viallon, C. Bordas, and J. Chevaleyre, J. Chem. Phys. **112**, 6228 (2000).
[19] G. Chen, Z. F. Liu, and X. G. Gong, Phys. Rev. B **67**, 205415 (2003).
[20] R. Car and M. Parrinello, Phys. Rev. Lett. **55**, 2471 (1985).
[21] M. C. Payne, M. P. Teter, D. C. Allan, T. A. Arias, and J. D. Joannopoulos, Rev. Mod. Phys. **64**, 1045 (1992).
[22] G. Kresse and J. Furthmüller, Phys. Rev. B **54**, 11169 (1996).
[23] D. Vanderbilt, Phys. Rev. B **41**, 7892 (1990).
[24] N. D. Mermin, Phys. Rev. A **137**, 1141 (1965).
[25] Q. Wang, Q. Sun, J.-Z. Yu, B.-L. Gu, Y. Kawazoe, and Y. Hashi, Phys. Rev. A **62**, 063203 (2000).
[26] A. R. Allouche, M. Aubert-Frécon, G. Nicolas, and F. Spiegelmann, Chem. Phys. **200**, 63 (1995).
[27] C. Kittel, *Introduction to Solid State Physics* (Wiley, New York, 1986).
[28] D. R. Lide, *CRC Handbook of Chemistry and Physics 1913-1995* (CRC, Boca Raton, Florida, 1995).
[29] B. Silvi and A. Savin, Nature (London) **371**, 683 (1994).
[30] A. D. Becke and K. E. Edgecombe, J. Chem. Phys. **92**, 5397 (1990).
[31] P. Labastie, J. M. Hermite, Ph. Poncharal, and M. Sence, J. Chem. Phys. **103**, 6362 (1995).
[32] G. Rajagopal, R. N. Barnett, A. Nitzan, U. Landman, E. C. Honea, P. Labastie, M. L. Homer, and R. L. Whetten, Phys. Rev. Lett. **64**, 2933 (1990).